A global picture of the seasonal persistence of stratospheric ozone anomalies

A global picture of the seasonal persistence of stratospheric ozone anomalies

S. Tegtmeier,[1,2] V. E. Fioletov,[1] and T. G. Shepherd[3]

Received 13 August 2009; revised 29 April 2010; accepted 8 June 2010; published 25 September 2010.

[1] Interannual anomalies in vertical profiles of stratospheric ozone, in both equatorial and extratropical regions, have been shown to exhibit a strong seasonal persistence, namely, extended temporal autocorrelations during certain times of the calendar year. Here we investigate the relationship between this seasonal persistence of equatorial and extratropical ozone anomalies using the SAGE-corrected SBUV data set, which provides a long-term ozone profile time series. For the regions of the stratosphere where ozone is under purely dynamical or purely photochemical control, the seasonal persistence of equatorial and extratropical ozone anomalies arises from distinct mechanisms but preserves an anticorrelation between tropical and extratropical anomalies established during the winter period. In the 16–10 hPa layer, where ozone is controlled by both dynamical and photochemical processes, equatorial ozone anomalies exhibit a completely different behavior compared to ozone anomalies above and below in terms of variability, seasonal persistence, and especially the relationship between equatorial and extratropical ozone. Cross-latitude-time correlations show that for the 16–10 hPa layer, Northern Hemisphere (NH) extratropical ozone anomalies show the same variability as equatorial ozone anomalies but lagged by 3–6 months. High correlation coefficients are observed during the time frame of seasonal persistence of ozone anomalies, which is June–December for equatorial ozone and shifts by approximately 3–6 months when going from the equatorial region to NH extratropics. Thus in the transition zone between dynamical and photochemical control, equatorial ozone anomalies established in boreal summer/autumn are mirrored by NH extratropical ozone anomalies with a time lag similar to transport time scales. Equatorial ozone anomalies established in boreal winter/spring are likewise correlated with ozone anomalies in the Southern Hemisphere extratropics with a time lag comparable to transport time scales, similar to what is seen in the NH. However, the correlations between equatorial and SH extratropical ozone in the 10–16 hPa layer are weak.

Citation: Tegtmeier, S., V. E. Fioletov, and T. G. Shepherd (2010), A global picture of the seasonal persistence of stratospheric ozone anomalies, *J. Geophys. Res.*, *115*, D18119, doi:10.1029/2009JD013011.

1. Introduction

[2] Stratospheric ozone exhibits strong interannual variability which can differ depending on latitude, altitude and season. Properly characterizing this variability and understanding its underlying mechanisms is important for detecting past trends and predicting future changes in stratospheric ozone, for validating models, and for combining different data sets.

[3] The vertical structure of ozone variability is linked to the boundary between dynamical and chemical control of ozone. Below ~28 km O_x has a long lifetime and ozone is controlled by transport processes, while above 30 km, O_x has a short lifetime and ozone is mainly controlled by chemistry. The narrow transition zone where ozone is influenced by both dynamics and chemistry is found between 28 and 30 km for tropical and extratropical regions and slopes slightly downward with increasing latitude in the summer hemisphere poleward of 40° [*Brasseur and Solomon*, 2005].

[4] Equatorial ozone variability is dominated by the quasi-biennial oscillation (QBO) in tropical zonal wind, with variability maxima in the lower (20–27 km) and middle/upper (30–37 km) stratosphere [*Zawodny and McCormick*, 1991; *Hasebe*, 1994]. The double peaked structure is related to the regions of dynamical and chemical control: the QBO signal in lower stratospheric ozone is forced by the transport of ozone via the QBO-induced meridional circulation, while the QBO signal in middle/upper stratospheric ozone arises from QBO related variability in temperature and in the transport of NO_y, both of which affect ozone chemically [*Ling and London*, 1986; *Zawodny and McCormick*, 1991; *Chipperfield et al.*, 1994; *Randel and Wu*, 1996; *Tian et al.*,

[1]Environment Canada, Toronto, Ontario, Canada.
[2]Now at Marine Meteorology, IFM-GEOMAR, Kiel, Germany.
[3]Department of Physics, University of Toronto, Toronto, Ontario, Canada.

0148-0227/10/2009JD013011

2006; *Tegtmeier et al.*, 2010]. The QBO ozone signals caused by ozone transport and by chemistry are of opposite phase and presumably cancel each other out in the transition zone between the dynamically and chemically controlled regions, which leads to a weak interannual ozone variability there.

[5] The QBO-induced ozone anomalies in the upper and lower stratosphere are in the same phase [*Randel and Wu*, 1996] and thus reinforce one another in terms of their effect on column ozone [*Bowman*, 1989; *Tung and Yang*, 1994]. This results from the opposite effect of the QBO on the local ozone concentration in the upper and lower stratosphere arising from the above mentioned opposite sign of the chemical and dynamical effects of the QBO-induced circulation anomalies, together with the fact that the QBO in the upper and lower stratosphere is generally in opposite phases at any given time.

[6] Latitudinal dependence of ozone variability is related to transport processes and their latitudinal and seasonal structure. In contrast to the tropics where the QBO signal completely dominates ozone variability, in the extratropics the ozone variability is largely driven by variability in the Brewer-Dobson circulation, which is mainly active in the winter–spring half of the year when the stratospheric winds are westerly. This imparts a very strong seasonal dependence to extratropical ozone variability [*Randel and Cobb*, 1994; *Randel and Wu*, 1996], including that associated with the QBO [*Tung and Yang*, 1994] which affects the dynamical forcing of the Brewer-Dobson circulation through the modulation of extratropical planetary-wave drag [*Holton and Tan*, 1980]. Over subtropical latitudes, the observed seasonal synchronization of the QBO ozone signal (which is only apparent in winter) is understood to arise in part from the hemispheric asymmetry of the QBO-induced meridional circulation, which is a consequence of nonlinear momentum advection [*Jones et al.*, 1998]. In particular, the thermally driven solstitial circulation in the tropics homogenizes the angular momentum distribution on the winter side of the equator [*Semeniuk and Shepherd*, 2001], inducing a stronger circulation response to the QBO.

[7] In addition to the seasonal dependence of the amplitude of ozone variability, it is also important to understand the temporal correlation structure of the ozone anomalies as this is a key parameter in trend detection and in validation of measurements. Because of the marked annual cycle of stratospheric dynamics, the temporal correlations in the extratropics can be expected to exhibit a seasonal dependence. *Fioletov and Shepherd* [2003] showed that midlatitude total ozone anomalies establish in winter/spring and then persist through the entire summer half of the year until the next autumn. The persistence is caused by the slow chemical decay of total ozone anomalies in the dynamically quiescent summer stratosphere. The anomalies are rapidly erased when the next winter's ozone buildup begins due to the onset of transport processes reflecting the next year's interannual variability. This mechanism applies to the partial ozone column below 28 km which is under dynamical control and which contributes, on average, 75% of the total ozone column. Surprisingly, *Tegtmeier et al.* [2008] found that the Northern Hemisphere (NH) subtropical partial ozone column above 28 km shows especially strong seasonal anomaly persistence, in spite of the short O_x lifetime in this chemically controlled region. Based on the analysis of other long-lived trace species, the study argued that the observed persistence of ozone anomalies arises from the summertime persistence of transport-induced wintertime anomalies in NO_y, which perturb ozone through NO_x chemistry. This seasonal persistence is distinct from the known QBO effect on upper stratospheric subtropical ozone via transport of NO_y, as it is asynchronous with the QBO while the latter is synchronous.

[8] In the equatorial region, there is no "dynamically quiescent summertime" and the QBO signal which dominates equatorial ozone variability is not synchronized with the annual cycle [*Baldwin et al.*, 2001]. However, it turns out that ozone anomalies in both the lower (40–25 hPa) and the middle/upper (6–4 hPa) equatorial stratosphere exhibit a seasonally dependent persistence between November and the following June, which arises from a previously unrecognized seasonal persistence of the QBO itself [*Tegtmeier et al.*, 2010]. In contrast to extratropical ozone anomalies which are affected by the QBO in an asynchronous manner during summer and early autumn, lower and middle/upper equatorial ozone anomalies are highly correlated with equatorial winds through the whole year.

[9] Equatorial ozone anomalies in the transition zone between the dynamically and chemically controlled regions show a strong seasonal persistence for a quite different time frame (June to December), which cannot be explained by the seasonal persistence of zonal wind anomalies [*Tegtmeier et al.*, 2010]. Ozone in this transition zone is of particular interest since this region serves as the primary supply region of ozone to the extratropical lower stratosphere [*Brasseur and Solomon*, 2005].

[10] The purpose of this study is to investigate whether extratropical ozone anomalies and their seasonal persistence are directly related to equatorial ozone anomalies. We focus our analysis mainly on the transition zone, but for completeness, we also investigate the dynamically and chemically controlled regions. We analyze the seasonal persistence of ozone anomalies in various layers and latitude bands using the same approach as *Fioletov and Shepherd* [2003]. Data sets and methods are described in section 2. In section 3, ozone anomalies in the lower and upper stratosphere are analyzed, while section 4 focuses on ozone anomalies in the transition zone. A summary and discussion of potential practical applications of seasonal persistence of anomalies, including multiple linear regression modeling, are provided in section 5.

2. Data and Methods

2.1. SAGE-Corrected SBUV Ozone Data Set

[11] The estimation of seasonal persistence of ozone anomalies requires long-term time series of ozone profile data. Such time series are provided by satellite instrument measurements like the Solar Backscatter Ultraviolet instrument (SBUV, SBUV/2) and the Satellite Aerosol and Gas Experiment (SAGE). The daily nearly global coverage of the first, and the precision and stability of the second, have been combined in the SAGE-corrected SBUV ozone data set [*McLinden et al.*, 2009], which is the primary data set analyzed here.

[12] The SBUV and SBUV2 instruments provide measurements of the ozone distribution with daily near-global

coverage from 1978 to present. The instruments were flown on a sequence of NOAA satellites (7, 9, 11, 14, 16, 17, and 18). Differences between the individual SBUV(/2) instruments lead to biases between the corresponding time series during the overlapping periods [*Frith et al.*, 2004]. Removing those biases has proven to be a challenge since the overlapping periods are sometimes short and the biases vary with time. The stratospheric SBUV(/2) ozone data are provided with a vertical resolution of about 3.2 km. It has been shown that the SBUV algorithm can cause a damping of ozone fluctuations with fine vertical structure [*Bhartia et al.*, 2004]. This is likely the explanation for the fact that the expected downward propagation of the equatorial QBO ozone signal is not properly captured in the SBUV(/2) data sets [*McLinden et al.*, 2009]. The biases between the individual SBUV data sets can be corrected with the help of a high quality ozone data set from a stable source spanning roughly the same time frame as the SBUV(/2) data sets. Such data is provided by the SAGE I and SAGE II data sets.

[13] The SAGE measurement technique [*McCormick et al.*, 1989; *Zawodny and McCormick*, 1991] is based on solar occultation providing ozone profile measurements that extend from the upper troposphere into the lower mesosphere. The measurements were obtained by the SAGE II sensor aboard the Earth Radiation Budget Satellite (ERBS) at sunrise and sunset on each of 14 orbits per day. Data records for the tropics and/or midlatitudes have substantial gaps for individual months of the year since spatial sampling is limited due to the satellite orbit. Validation studies have demonstrated the good quality of the SAGE I and SAGE II data records with an estimated precision of around 10% for SAGE I and 4–8% for SAGE II [*Cunnold et al.*, 1989; *Fioletov et al.*, 2006].

[14] Coincident measurements by SAGE and SBUV(/2) were identified if they occurred on the same day and within 1000 km of each other [*McLinden et al.*, 2009]. Differences between the coincident measurements were used for a bias correction of the individual SBUV(/2) instruments. The resulting new data set is called the SAGE-corrected SBUV data set and is based on SBUV(/2) data version 8.0 [*Bhartia et al.*, 2004], SAGE I version 7.0, and SAGE II version 6.2 [*Wang et al.*, 2006]. As an important result of the corrections, the new data set shows a realistic downward propagation of the equatorial QBO ozone signal, in contrast to the original SBUV(/2) time series. The SAGE-corrected SBUV data set consists of monthly zonal means and spans the time period from 1978 to 2005, limited by the end of SAGE II operations. For 12 layers, each approximately 3.2 km thick, the provided quantity is the partial ozone column (DU). The zonal mean ozone profiles provided in 5° wide latitude bands cover 80°S–80°N. Tropical ozone data is excluded for the time period of a year following the eruption of El Chichon, and following the eruption of Mt. Pinatubo.

2.2. HALOE Data Set

[15] The Halogen Occultation Experiment (HALOE) instrument [*Russell et al.*, 1993] aboard the Upper Atmosphere Research Satellite (UARS) observed mixing ratios of a number of trace gases including NO and NO_2 from 1991 to 2005. The measurement technique is based on solar occultation with daily observations of up to 15 sunrise and 15 sunset profiles. The observations cover up to 80° during spring/summer of the respective hemisphere and up to 50° for the rest of the year. In this study we use NO_x profiles, which are calculated as the sum of the measured NO and NO_2, to analyze the seasonal persistence of NO_x anomalies. The HALOE data set used here consists of monthly mean values covering the time period from October 1991 to August 2002 prepared by *Grooß and Russell* [2005]. The observations were much less frequent after 2002 and therefore the most recent data have not been included in this data set. The data are averaged over 5° wide equivalent latitude bins. The mixing ratio profile of NO_x is based on sunset events only and given for 22 pressure levels between 316 and 0.1 hPa.

2.3. Methods

[16] The temporal persistence of ozone anomalies can be quantified by the strength of the correlation between the ozone anomalies in one month and the anomalies in another month. In order to determine the seasonal dependence of this temporal persistence, we calculate the correlations between time series of partial ozone columns for individual months and latitude bands following the approach introduced by *Fioletov and Shepherd* [2003]. Let x and y be the partial ozone column in two particular months, latitude bands and layers. The correlation coefficient between x and y equals

$$r_{xy} = \frac{\sum_{i=1}^{n-k} x_i y_{i+k}}{\sqrt{\sum_{i=1}^{n-k} x_i^2}\sqrt{\sum_{i=1}^{n-k} {y_{i+k}}^2}},$$

where x_i and y_{i+k} are the ozone anomalies in year i and year $i + k$, respectively, and n is the number of years in the record. Correlation coefficients between the 27 year time series greater than 0.4 are statistically significant at the 95% confidence level based on the Student's t test.

[17] The seasonal cycle and the long-term trend associated with the amount of ozone depleting chlorine and bromine in the stratosphere are removed from the original data prior to the calculation of the correlation coefficients. The long-term ozone change is estimated by fitting the ozone time series to the equivalent effective stratospheric chlorine (EESC) loading. The EESC function is a measure of the stratospheric halogen burden [e.g., *Newman et al.*, 2007] and its loading is chosen corresponding to the layer and latitude region of the examined ozone anomalies. The long-term trend is estimated separately for each month of the year.

[18] A statistical regression analysis of the SAGE-corrected SBUV ozone data set is used to demonstrate that the seasonal persistence can help to improve the explanatory power of multiple linear regression models. For this application, which is used only to supplement the main analysis, the ozone time series for each month were fit with a regression model including EESC, solar cycle, and QBO as explanatory variables [*World Meteorological Organization*, 2007, and references therein]. The QBO time series are based on observed equatorial winds at 30 hPa and 50 hPa, and the solar cycle term is the standard $F_{10.7}$ radio flux. The regression model includes a constant and an annual harmonic term for the regression coefficients of the EESC and QBO function. The regression model is applied to the ozone

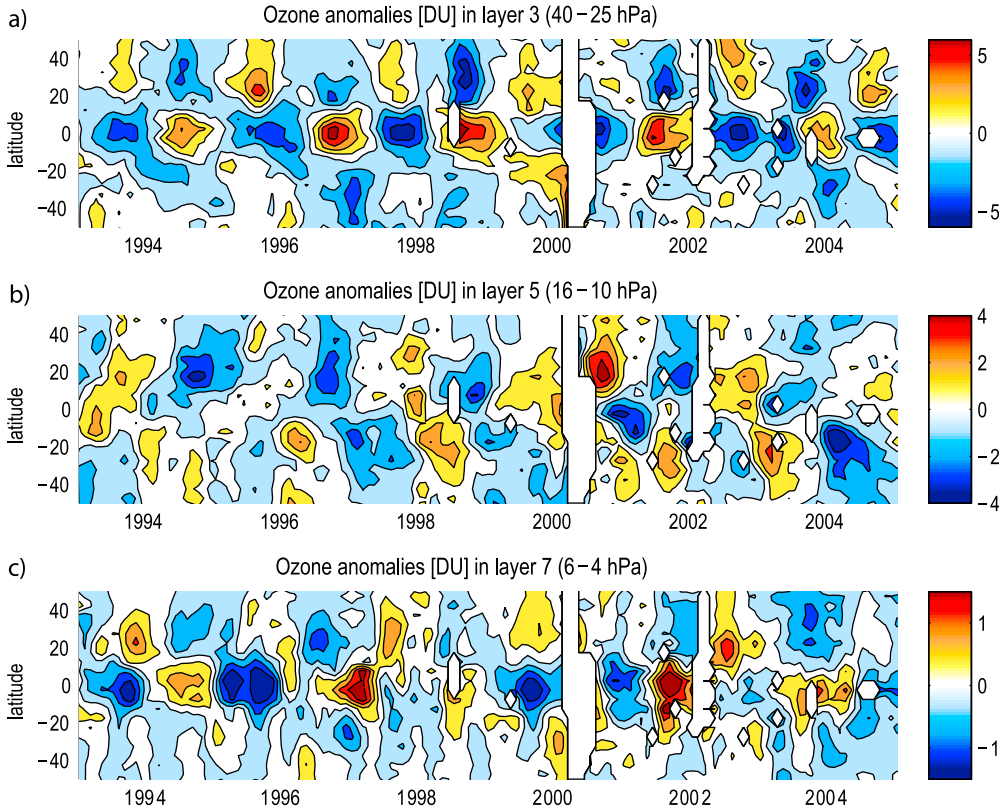

Figure 1. Latitude-time section of interannual ozone anomalies from 1993 to 2005 from the SAGE-corrected SBUV data set for (a) layer 3 (40–25 hPa), (b) layer 5 (16–10 hPa), and (c) layer 7 (6–4 hPa).

time series of each month separately. We construct a second regression model by replacing the instantaneous QBO time series as explanatory variables by QBO time series corresponding to a certain time of the calendar year. Whereas the standard regression model applied to ozone in the month x uses the equatorial winds in the same month x, the new regression model uses the equatorial winds in November/December. In particular, for every month from January up to September the equatorial winds in November/December of the previous year are used, and for the months between October and December the equatorial winds in November/December of the same year are used.

3. Ozone Variations in the Lower and Upper Stratosphere

[19] As discussed in section 1, upper and lower stratospheric ozone anomalies in the equatorial region, and in the NH subtropics, show a seasonal persistence from boreal autumn until early summer (or into autumn in the subtropical upper stratosphere) of the following year. It is of interest to investigate whether the ozone anomalies in the tropics and subtropics, and the mechanisms driving their seasonal persistence, are somehow connected.

[20] In order to address this topic, we focus on the behavior of ozone in two specific layers representing the lower and upper stratosphere. Figure 1 shows latitude-time sections of interannual ozone anomalies derived from the SAGE-corrected SBUV data set. For clarity, only the portion from 1993 to 2005 of the 27 year long data set is displayed. The seasonal cycle and the EESC trend have been removed from the monthly zonal mean ozone data for each 5 degree wide latitude band. Here we will only discuss the ozone anomalies in layer 3 (corresponding to the partial ozone column between 40 and 25 hPa, Figure 1a) and layer 7 (6–4 hPa, Figure 1c), while the ozone anomalies in layer 5 (16–10 hPa, Figure 1b) are discussed in section 4. The variability of tropical ozone (10°S–10°N) in both layers 3 and 7 is dominated by the QBO with its characteristic alternating positive and negative anomalies [*Zawodny and McCormick*, 1991; *Hasebe*, 1994]. The QBO signal in extratropical ozone is seasonally synchronized, and shows maxima in winter/spring in each respective hemisphere [*Randel and Wu*, 1996]. An important aspect of the global QBO pattern is that the tropical and extratropical ozone anomalies are approximately 180° out of phase.

[21] Figure 2 shows the correlation coefficients between the monthly mean ozone time series for layer 3 and layer 7, averaged over the latitude bands 0°N–10°N, 10°N–20°N and 20°N–40°N. In the equatorial region (Figure 2, left) both layers are characterized by a seasonal persistence of the interannual anomalies from autumn/early winter to spring/early summer, i.e., the ozone anomalies between any two months within this time frame are highly correlated. In the subtropical region (Figure 2, right) the correlation coefficients for the lower and the upper stratosphere show similar

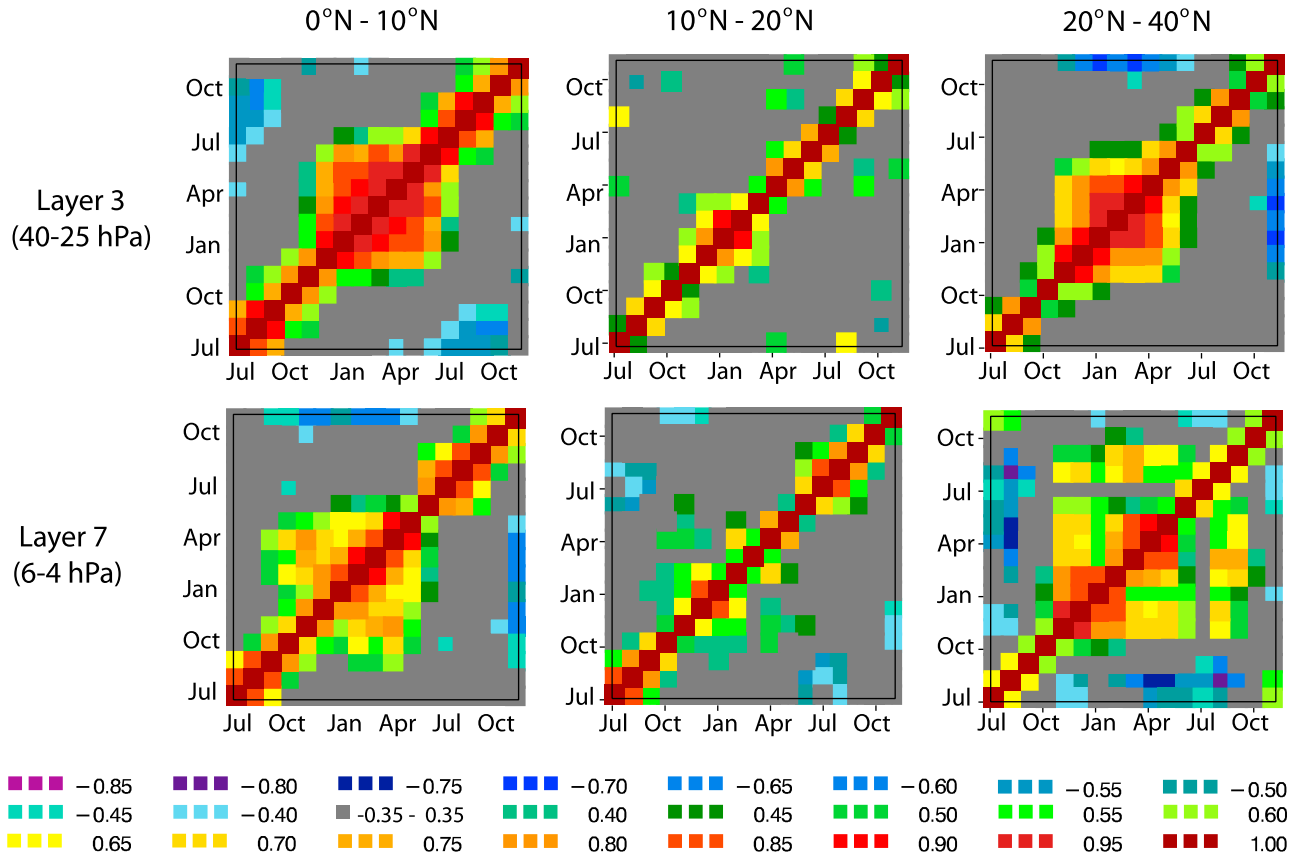

Figure 2. Correlation coefficients between monthly mean ozone time series of the SAGE-corrected SBUV data set averaged over the regions 0°N–10°N, 10°N–20°N, and 20°N–40°N for (top) layer 3 (40–25 hPa), and (bottom) layer 7 (6–4 hPa). Each field represents the correlation between the ozone time series for two particular months, as labeled.

patterns, with high coefficients between November and June or September, respectively.

[22] We find strong positive correlations (with coefficients between 0.5 and 0.85) between ozone anomalies in the upper and lower stratospheric layers within, but only within, their time frame of seasonal persistence: in both regions, tropics and subtropics, anomalies in layer 3 and layer 7 are well correlated during the months from November to June, but not before or after that.

[23] The picture changes completely if we look at the intermediate latitude region, 10°N–20°N (Figure 2, middle). For both layers, no statistically significant correlations between anomalies separated by more than 2–3 months can be found. As noted earlier the QBO ozone signals in the equatorial region and in the subtropics are 180° out of phase, and the transition zone where they cancel each other out is approximately between 10°N and 20°N (see also Figure 3). As a result, the variability of ozone anomalies in this latitude band is weak compared to the variability of equatorial or subtropical ozone anomalies.

[24] Ozone anomalies in the Southern Hemisphere (SH) subtropics display only a very weak persistence (not shown here). This might be just a problem of detectability given the shortness of the data record, as the SH subtropical anomalies are much weaker (by roughly a factor of 2) compared to the NH. The fact that the SH subtropical ozone anomalies are substantially weaker than those in the NH points to the importance of processes other than the direct QBO-induced circulation in inducing subtropical ozone variability in layers 3 and 7. In particular, it is well known that the Brewer-Dobson circulation is much weaker in the SH [e.g., *Shepherd*, 2007]. Given the lack of a statistically significant signal in the SH, we focus our analysis of lower and upper stratospheric ozone anomalies on the tropical and NH extratropical regions.

[25] We now explore how the lower stratospheric ozone anomalies in the different latitude bands are related to each other. Figure 3a shows the correlation coefficients between equatorial ozone anomalies in October and ozone anomalies in the latitude band and month labeled by the x and y axis, respectively. (To facilitate interpretation of Figure 3a, the reference cell, representing the correlation of the time series of equatorial ozone in October with itself and therefore showing the value unity, is framed in white.) Equatorial ozone anomalies in layer 3 in October do not show any strong correlation with extratropical ozone anomalies during the rest of the year. Note that October is 2 months before the start of the timeframe of seasonal persistence of equatorial ozone anomalies in layer 3 (seen in Figure 2). The picture changes completely if we use ozone anomalies in December instead of October as the reference time series (Figure 3b). Now ozone anomalies in the tropics and extratropics are of

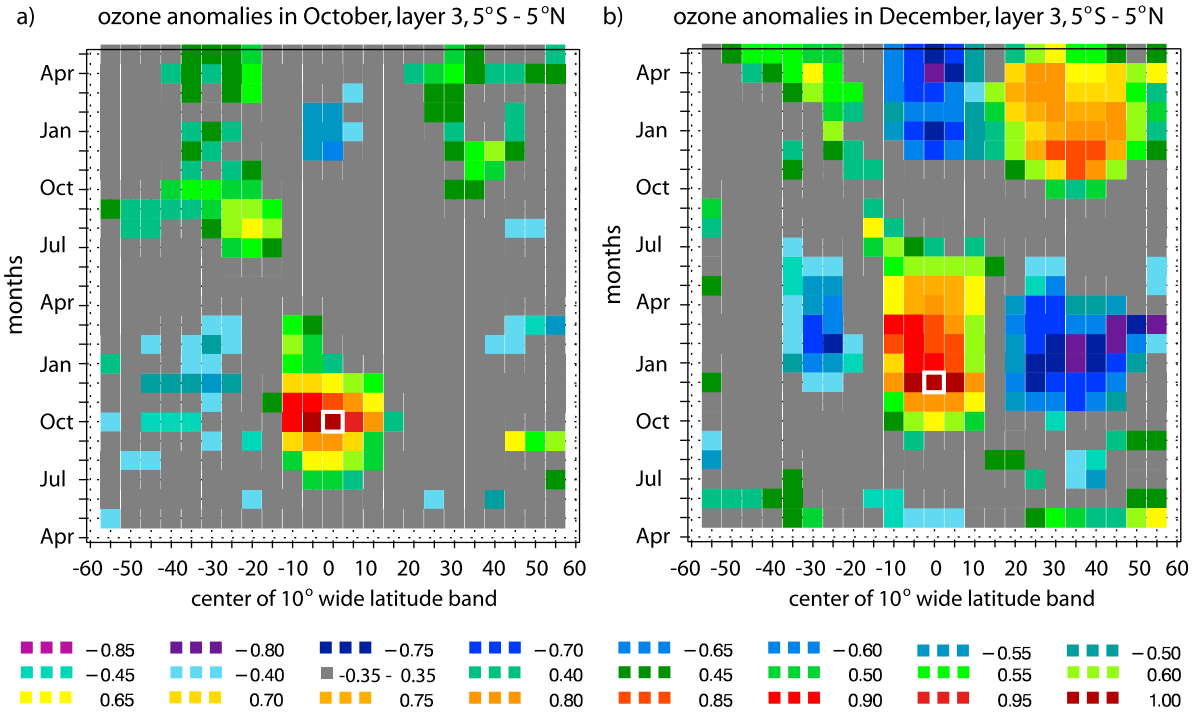

Figure 3. Correlation coefficients between monthly mean ozone time series in layer 3 (40–25 hPa) for the month and latitude band as labeled and ozone anomalies for layer 3 averaged over the region 5°S–5°N for (a) October and (b) December. Data are taken from the SAGE-corrected SBUV data set.

opposite sign, as demonstrated by their instantaneous anticorrelations. Comparison of Figures 3a and 3b indicates that equatorial ozone anomalies during, and only during, the months of their seasonal persistence (which is apparent from Figure 2) are anticorrelated with ozone anomalies in the NH extratropics. This is confirmed by further test cases (not shown here) with ozone anomalies in different months as reference time series. The opposite sign of the ozone anomalies in the equatorial region and subtropics during the wintertime reflects the QBO-induced vertical circulation which has opposite effects in the equatorial region and the subtropics, and which maximizes in winter [*Jones et al.*, 1998]. However, in the lower stratosphere the ozone lifetime is sufficiently long that the transport-induced subtropical signal persists for several more months, into early summer. Advection by the Brewer-Dobson circulation allows this subtropical signal to propagate into midlatitudes during the winter/early spring period, but the signal is then presumably diluted by other sources of variability, including the influence of polar variability [*Fioletov and Shepherd*, 2005].

[26] To complete our analysis of ozone correlations between different latitude bands, we calculated the correlation coefficients for layer 7 (not shown here) in a manner analogous to the calculation for layer 3. We know that the ozone anomalies in layer 7 are characterized by very similar persistence compared to the ozone anomalies in layer 3 in both tropical and NH extratropical regions. The correlations between varying latitude bands and months for layer 7 show the same pattern as that seen for layer 3 (Figure 3): equatorial ozone anomalies are anticorrelated with the NH extratropical ozone anomalies only during the time frame of persistence in both regions.

[27] Overall, the characteristic of having strong anticorrelations between tropical and NH subtropical ozone anomalies only during the time frame of their seasonal persistence has been found for both the upper and lower stratosphere. However, in both cases the anticorrelation only indicates a synchronous relationship during the winter season. The anticorrelation between tropical and subtropical ozone anomalies in the spring and early summer results from the separate seasonal persistence of the equatorial and subtropical anomalies, each arising from entirely different mechanisms. In the equatorial region the anomaly persistence results from the persistence of the QBO itself [*Tegtmeier et al.*, 2010], while in the subtropics it results from the persistence of the ozone (lower stratosphere) or NO_y (upper stratosphere) anomalies established during winter [*Tegtmeier et al.*, 2008].

4. Ozone Variations Between 16 and 10 hPa

[28] We now focus on ozone anomalies in layer 5, corresponding to the partial ozone column between 16 and 10 hPa. Ozone in layer 5 is of particular interest since the transition between the dynamically and chemically controlled regions is located here, which serves as the primary supply region of ozone to the extratropical lower stratosphere [*Brasseur and Solomon*, 2005]. The maximum in the vertical profile of tropical ozone mixing ratio occurs between 15 and 5 hPa, with layer 5 (16–10 hPa) being part of this region. Equatorial ozone anomalies in layer 5 are characterized by a seasonal persistence from June/July to December [*Tegtmeier et al.*, 2010]. On the other hand, the NH sub-

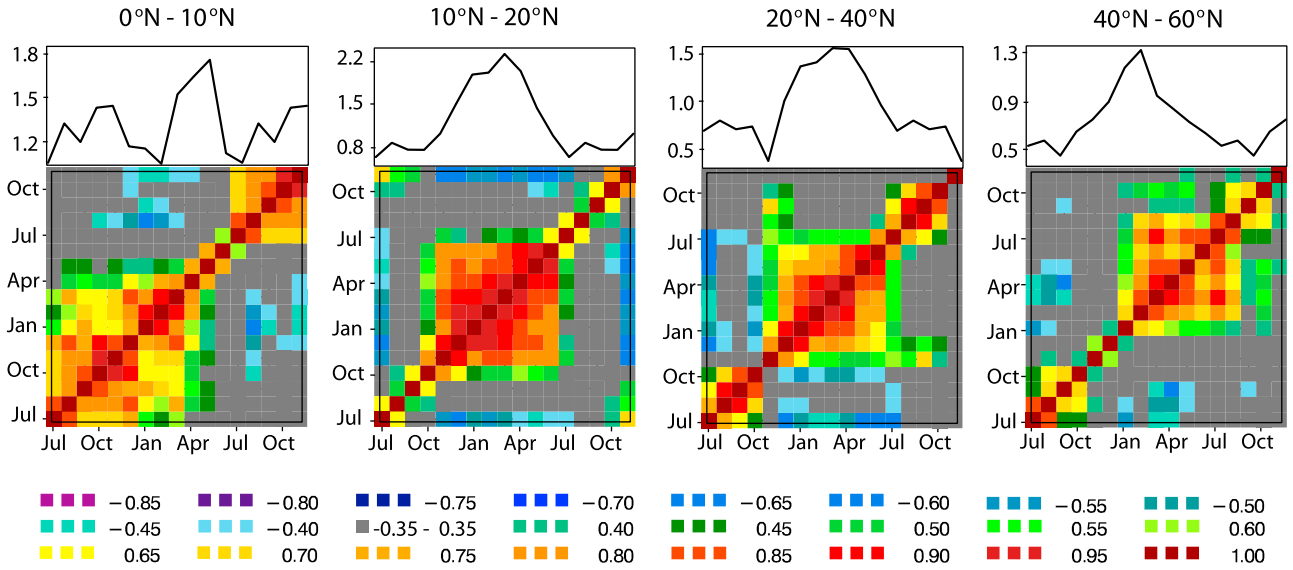

Figure 4. (top) Seasonal cycle of the standard deviation of ozone anomalies and (bottom) correlation coefficients between monthly mean ozone anomalies for layer 5 of the SAGE-corrected SBUV data set for the regions 0°N–10°N, 10°N–20°N, 20°N–40°N, and 40°N–60°N. Each field represents the correlation between the ozone time series for two particular months, as labeled.

tropical ozone anomalies above 16 hPa show a very strong seasonal persistence from late autumn until early autumn of the following year [*Tegtmeier et al.*, 2008]. Here we explore how the persistence of equatorial and extratropical ozone anomalies are related to each other.

[29] Figure 1b shows the latitude-time section of interannual ozone anomalies derived from layer 5 of the SAGE-corrected SBUV data set. Tropical ozone anomalies in layer 5 are largely independent of the QBO signal [*Tegtmeier et al.*, 2010]. Moreover, tropical and NH extratropical ozone anomalies are generally not out of phase as is the case for layers 3 and 7. In particular, for a large number of years it seems that the equatorial ozone signal shows up in the NH extratropical region lagged by only a few months, and in the SH extratropical region lagged by at least 6 months. It seems possible that the equatorial and NH extratropical ozone anomalies in layer 5 are directly connected by horizontal transport.

[30] Figure 4 shows standard deviations and the correlation coefficients between the monthly mean ozone time series for layer 5 for the latitude bands 0°N–10°N, 10°N–20°N, 20°N–40°N, and 40°N–60°N derived from the SAGE-corrected SBUV ozone data set. The equatorial region and the two extratropical latitude bands show the expected seasonal persistence of anomalies. Surprisingly, ozone anomalies in the latitude band 10°N–20°N are characterized by a very strong seasonal persistence as well, in contrast to the ozone anomalies in layer 3 and layer 7 for this latitude band. In general, for all four latitude bands shown in Figure 4, there exists a time frame during which the correlation coefficients between the monthly mean ozone time series of layer 5 are very high, whereas before and after the time frame the correlations are not statistically significant. Interestingly, the time frame of seasonal persistence shifts to a later time of year for higher latitudes. In the region 0°N–10°N, we find strong memory from July to March, which starts at the same time as the memory in the equatorial region 5°S–5°N but lasts 3 months longer. For the latitude band 10°N–20°N, there is strong memory from November until June, with all the correlation coefficients between the eight monthly mean ozone time series of the time frame being larger than 0.8. There is a shift by 1 month between this time frame and that found for the midlatitude band 20°N–40°N. Finally, the region 40°N–60°N shows strong seasonal persistence from February until August. Overall, the time frame of strong seasonal persistence shifts by approximately 6 months from the equatorial regions to the high midlatitudes. Analysis of the seasonal cycle of the standard deviations of ozone anomalies illustrates that in the two latitude bands between 10°N and 40°N the time frames of seasonal persistence and of large ozone variability are nearly identical. However, for 40°N–60°N the peak of ozone variability happens at the same time as the start of the seasonal persistence. Overall, seasonal persistence and the magnitude of ozone variability appear to be linked in the regions north of 10°N but there exists no clear one-to-one relationship.

[31] *Tegtmeier et al.* [2008] argued that the seasonal persistence of the subtropical partial ozone column between 16 and 1.6 hPa is caused by the persistence of transport-induced NO_y anomalies which influence ozone through NO_x chemistry. Although layer 5 is generally located between the dynamically and chemically controlled regions, it seems possible that there exists a persistence of transport-induced NO_y (and hence NO_x) anomalies which is causing the persistence of ozone anomalies for middle stratospheric layers around 16–10 hPa.

[32] In order to test this hypothesis we look into HALOE NO_x measurements. Figure 5 shows the year to year variability of HALOE NO_x anomalies at 10 hPa averaged over each of the four latitude bands used in Figure 4. Each plot of Figure 5 displays for one latitude band the time series of the individual months corresponding to the time frame of strong

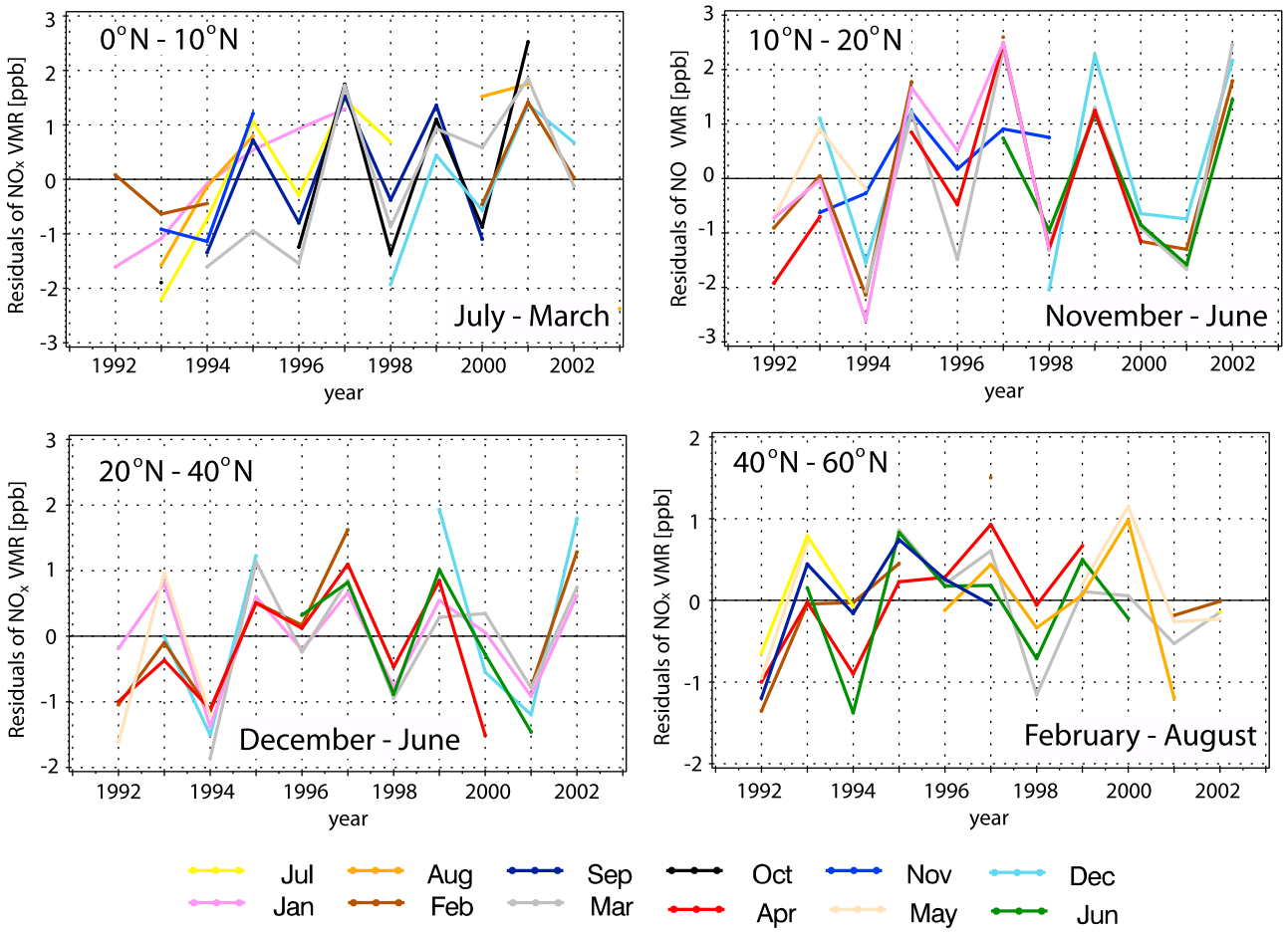

Figure 5. Time series of NO_x anomalies at 10 hPa for every month between (top left) July and March averaged over 0°N–10°N, (top right) November and June averaged over 10°N–20°N, (bottom left) December and June averaged over 20°N–40°N, and (bottom right) February and August averaged over 40°N–60°N equivalent latitude.

seasonal persistence of layer 5 ozone anomalies. In general, the number of years is too small to calculate meaningful correlation coefficients between the time series, as was done for the ozone anomalies. However, the NO_x anomalies clearly persist during the time frame chosen for the particular latitude band. NO_x anomalies before and after the time frame (not shown here) do not match the pattern of interannual variability of the NO_x time series within the time frame, i.e., for 10°–20° equivalent latitude the time frame of persistence starts in November and the NO_x anomalies for September or October show a completely different variability than the time series for November and the following months. Overall, the NO_x anomalies at 10 hPa persist during time frames nearly identical to those found for ozone anomalies between 16 and 10 hPa.

[33] Since the NO_x anomalies are defined for a given latitude, altitude, and time of year, they will be mainly associated with NO_y anomalies. (The time scale of persistence is too long to be associated with temperature anomalies, given the short radiative damping times in the upper stratosphere.) Therefore it is reasonable to hypothesize that seasonal persistence of NO_y anomalies, which is characterized by a strong latitudinal dependence, is causing the same characteristics in ozone anomalies through perturbed NO_x catalytic cycles. On the other hand, the anomalous NO_y may just reflect an anomalous circulation which affects ozone directly; a stronger Brewer-Dobson circulation would be expected to increase ozone through transport and also via reduced NO_y (since age-of-air would be younger). Either mechanism or a combination of the two can provide a possible explanation for the persistence of the ozone anomalies in this region. Since they act coherently, probably model studies are required to separate the two effects.

[34] Figure 6 shows the correlation coefficients for ozone anomalies in layer 5 for four latitude bands of the SH. In a manner similar to the NH, each latitude band shows a time frame during which the correlation coefficients between the monthly mean ozone time series are very high. The strongest seasonal persistence can be found for 10°S–20°S (May–December) and for 20°S–40°S (June–April). Note that for the midlatitude band 20°S–40°S the persistence extends over nearly a year. The tropical SH latitude band 0°S–10°S shows a seasonal persistence which is similar to its NH counterpart but which ends earlier. For the latitude band 10°–20°, the NH and SH are almost exactly 6 months out of phase. As in the NH, the time frame of high correlation coefficients shifts to a later time of year as one moves from 10°S–20°S into the extratropics.

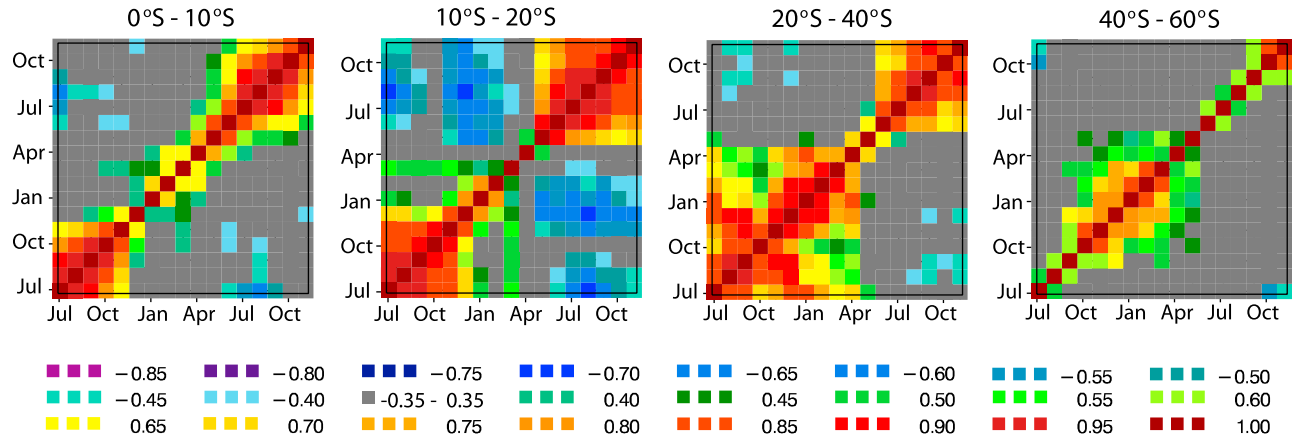

Figure 6. Same as Figure 4 (bottom) but for the SH.

[35] To investigate further how layer 5 ozone anomalies in the different latitude bands are related to each other we calculate correlations between ozone time series in varying latitude bands and months. Figure 7a shows the correlation coefficients between ozone anomalies averaged over 5°S–5°N in May and ozone anomalies in the latitude band and month labeled by the *x* and *y* axis, respectively. Apparently, middle stratospheric (16–10 hPa) equatorial ozone anomalies in May are only weakly correlated with ozone anomalies in the SH subtropics 2–3 months later, and there are no significant correlations with any NH middle stratospheric ozone anomalies. However, May is 1 month before the start of the timeframe of seasonal persistence of equatorial ozone anomalies in layer 5 [*Tegtmeier et al.*, 2010]. The picture changes completely if we use ozone anomalies in July instead of May as a reference time series (Figure 7b). Now we find very strong correlations between equatorial ozone and ozone in the NH extratropical region. Ozone anomalies in the tropics and NH extratropics are positively correlated, but not instantaneously, only with a time lag of 3 to 6 months. In any particular tropical and NH latitude band, significant correlations occur only where the seasonal persistence of anomalies was found (Figure 4). Additionally, high positive correlations between the tropics and the SH extratropics lagged by approximately 1–1.5 years are evident in Figure 7b. Further analysis, based on reference months from the time frame of strong seasonal persistence of equatorial ozone anomalies (July–December), shows a very similar picture with time lagged correlations between the tropics and NH extratropics (3–6 months), and between the tropics and SH extratropics (1 year). This is confirmed by Figure 7c showing the correlations based on the reference month November. If we choose a reference month which is not part of the time frame of high seasonal persistence then there are no correlations between the tropics and the NH extratropics and only weak correlations between the tropics and the SH extratropics lagged by 3–6 months, as in Figure 7d based on the reference month of January.

[36] Overall we can conclude that middle stratospheric ozone anomalies in layer 5 in the tropics and in the NH extratropics are strongly correlated, but only in their respective time frames of seasonal persistence. This suggests that equatorial ozone anomalies established in boreal summer/autumn are mirrored in the ozone anomalies in the extratropical NH with a time lag of a few months, which is similar to transport time scales. Equatorial ozone anomalies established in boreal winter/spring are likewise correlated with ozone anomalies in the SH extratropics with a time lag comparable to transport time scales, similar to what is seen in the NH. However, these correlations between equatorial and SH extratropical ozone are weak, and overall the SH ozone variability is dominated by a signal based on 1 year time lagged anticorrelations in the extratropics. In the NH extratropics, on the other hand, the 1 year time lagged anticorrelations are not strong enough to dominate the signal from the tropics. The correlations between equatorial and extratropical ozone confirm our inferences made earlier based on the latitude-time section of ozone anomalies in layer 5 (Figure 1b).

5. Summary and Discussion

[37] Analysis of ozone data, in the regions of the stratosphere where ozone is purely dynamically or purely chemically controlled, has demonstrated that there is no apparent relation between the seasonal persistence of tropical and NH extratropical ozone anomalies. However, ozone in the layer between chemical and dynamical control shows some very interesting characteristics, which point to a direct link between tropical and extratropical ozone anomalies.

[38] Tropical ozone anomalies in the lower and upper stratosphere persist from boreal autumn until spring/early summer of the following year. NH extratropical ozone anomalies show a quite similar seasonal persistence, although it apparently results from different mechanisms. Our analysis shows that the well-known instantaneous anticorrelations between tropical and extratropical ozone anomalies are only observed during the time frame of their seasonal persistence. The extent to which this is a coincidence is unclear. Within the winter season, the anticorrelation of tropical and subtropical ozone anomalies is explainable from the seasonal asymmetry of the QBO-induced vertical circulation, which maximizes during winter [*Jones et al.*, 1998]. However, the anticorrelation during spring/early summer arises from the separate seasonal persistence of the tropical and subtropical signals, from apparently different mechanisms.

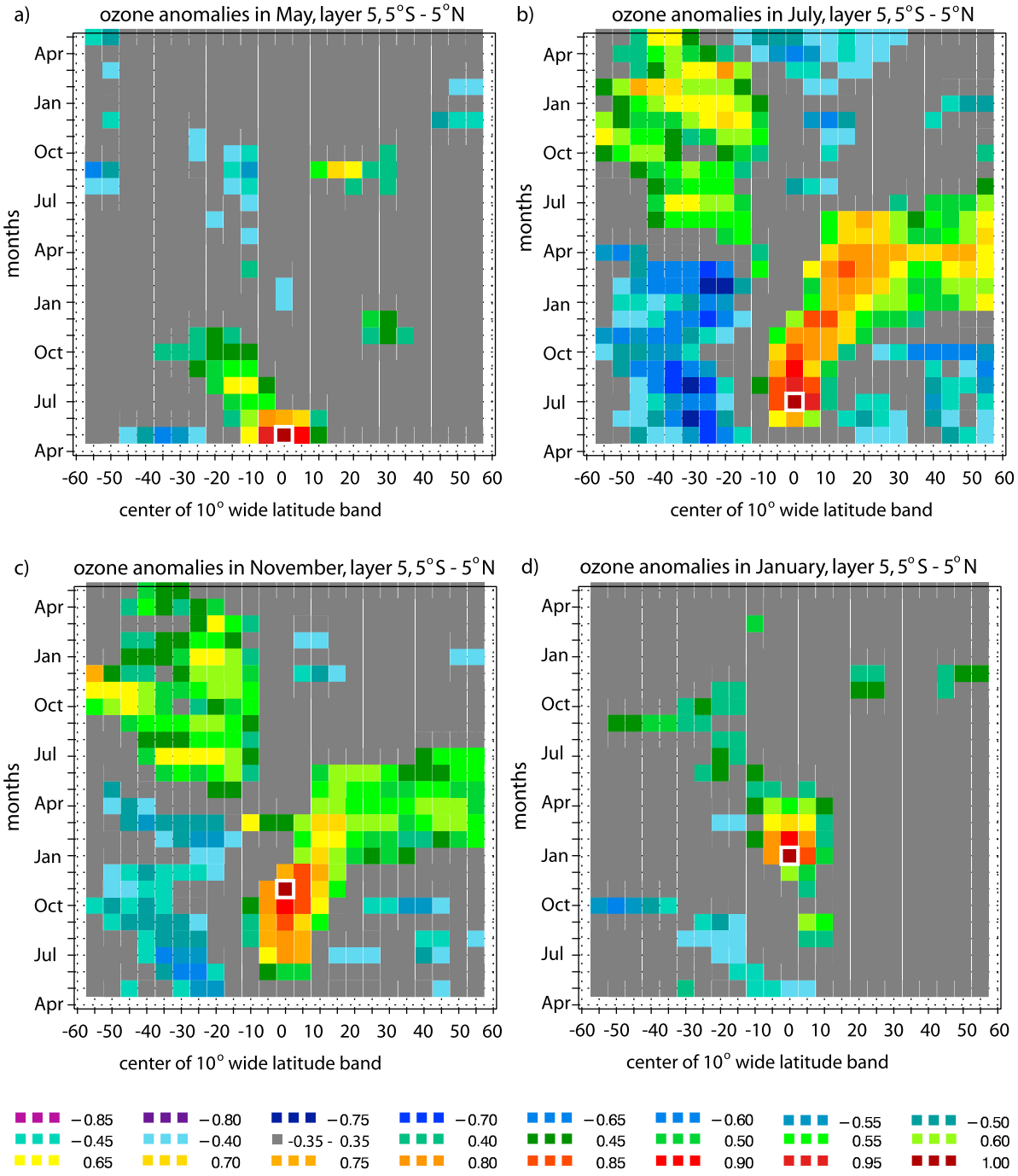

Figure 7. Correlation coefficients between monthly mean ozone time series in layer 5 (16–10 hPa) for the month and latitude band as labeled and ozone anomalies for layer 5 averaged over the region 5°S–5°N for (a) May, (b) July, (c) November, and (d) January. Data are taken from the SAGE-corrected SBUV data set.

[39] Between the two tropical stratospheric layers of maximum ozone variability, ozone anomalies are small and less dominated by the QBO signal. The analysis of equatorial ozone anomalies in this stratospheric region (16–10 hPa) demonstrates a strong seasonal persistence from June to December, almost exactly complementary to the timeframe of seasonal persistence in the upper and the lower stratosphere. The reasons for this are not understood. Extratropical ozone anomalies in the same layer are characterized by a very similar seasonal persistence with the time frame of persistence shifted by approximately 6 months when going from the equatorial region to high midlatitudes. Correlation coefficients between the anomalies in tropical and extratropical regions demonstrate that during a distinctive time of the calendar year (which equals the time frame of their respective seasonal persistence), ozone in the tropics shows

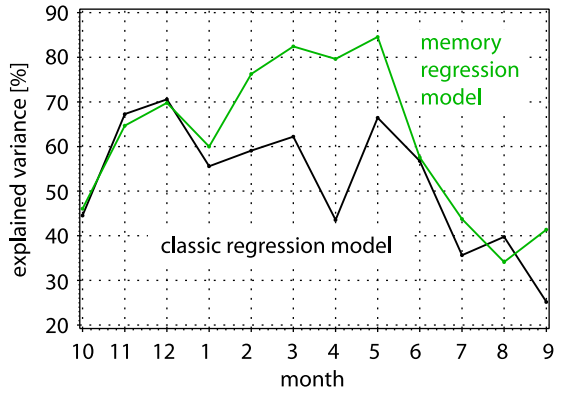

Figure 8. Variance (%) explained by regression models for ozone anomalies averaged over 10°N–20°N for 16–10 hPa from the SAGE-corrected SBUV data set. The regression models are based on instantaneous equatorial winds (black) and equatorial winds from the previous November/December (green).

the same variability as ozone in the NH extratropics, with the latter variability lagged by 3–6 months. During the time where equatorial ozone anomalies show no seasonal persistence, they are only weakly correlated with ozone anomalies in the SH extratropics. However, these correlations show a similar time lag of 3–6 months, which is comparable to transport time scales.

[40] Tropical ozone anomalies between 16 and 10 hPa thus exhibit completely different behavior compared to ozone anomalies above and below this level in terms of their variability, seasonal persistence, and relation to extratropical ozone. Above 10 hPa the variability of ozone is linked to the variability of NO_y through its impact on NO_x catalytic cycles, together with variability of temperature through the O_x cycles. Below 16 hPa, ozone is under dynamical control and mainly influenced directly by transport processes. It is plausible that NO_y transport from the equatorial region into the NH extratropics causes the correlations between tropical and NH extratropical ozone in layer 5 which are characterized by a time lag similar to transport time scales. In support of this hypothesis, it has been shown that NO_x anomalies at 10 hPa and ozone anomalies between 16 and 10 hPa in the tropics and NH extratropics show a very similar seasonal persistence. However, at these altitudes, transport processes could affect ozone directly and cause the high correlations during the time frames of seasonal persistence. Since both mechanisms affect ozone in the same way, it is not possible to distinguish them from observational analysis alone.

[41] Seasonal persistence of extratropical ozone anomalies in the upper stratosphere has been shown to be a potentially useful tool for filling data gaps [*Tegtmeier et al.*, 2008]. In this region, most of the ozone variability during summer and autumn can be described by the ozone variability in the previous winter/spring. Therefore, ozone variability can be estimated from available data in winter/spring and then used to reconstruct missing data during the rest of the year until autumn. This method of filling data gaps might be especially important for satellite ozone data sets based on the occultation method, where data records show substantial gaps for individual months of the year, or for the reconstruction of historical ozone data sets. Seasonal persistence of anomalies can also be used for the validation of chemistry climate models [*Tegtmeier and Shepherd*, 2007] or for the purpose of data validation.

[42] Another practical application of the results found in our study is that the strong seasonal persistence of ozone anomalies can help to improve the explanatory power of multiple linear regression models. Usually, regression models use the equatorial wind as an explanatory variable based on the assumption that the ozone signal represents a long-term variation related to the QBO signal with a period of about 28 months, modulated by the seasonal cycle. However, the correlations between equatorial wind and extratropical ozone are small in summer and autumn. Yet we know that upper stratospheric ozone variations in summer and autumn are related to those in winter and spring, and therefore related to the QBO signal in winter and spring. A possible way to improve the explanatory power of regression models in summer is to replace the instantaneous QBO as explanatory variable with a QBO term lagged by a certain amount of time, i.e., with the QBO signal from the previous winter.

[43] Figure 8 shows the output from two regression models, one a classical regression model based on the instantaneous QBO term and the other a new regression model based on the early winter QBO term. Both models are described in detail in section 2. The regression models were run for ozone anomalies between 16 and 10 hPa in the latitude band 10°N–20°N for each month separately. The black line represents the variance explained by the classical regression model based on the instantaneous QBO term, while the green line shows the variance explained by the new regression model based on the equatorial winds in November/December. During autumn and early winter both regression models explain the same amount of variance. Yet we know that the ozone anomalies averaged over 10°N–20°N persist from November until June (Figure 4). Especially in the second half of this time frame, the regression model based on the QBO winds from the previous early winter explains between 15% and 35% more variance than does the classical regression model. This is explained by the asynchronous effect of the QBO on extratropical ozone through "seasonal memory." Note that this technique can only help to improve the explanatory power of regression models in regions and times of year where the seasonal persistence is caused by the fact that the dynamical variability is weak. The same technique would not improve regression model performance in the tropical region where the seasonal persistence of ozone is caused by the seasonal persistence of the zonal winds themselves [*Tegtmeier et al.*, 2010] and the dynamical variability is not weakened during this time of year. During summer and autumn, both regression models explain only a small part of the variance of ozone anomalies. In the case of the "classical" regression model, this is due to the weak correlation between equatorial wind and extratropical ozone in summer and autumn [*Randel and Wu*, 2007]. In the case of the memory regression model, this is caused by the fact that the seasonal persistence lasts from November until June and only during this time frame can the ozone variability be explained by the QBO signal from the preceding early winter.

[44] **Acknowledgments.** The authors would like to thank the NASA Langley Research Center (NASA-LaRC) and NOAA for making SAGE, SBUV, and HALOE data available. S.T. especially acknowledges the Canadian Natural Sciences and Engineering Research Council postdoctoral fellowship allowing this study to be completed. T.G.S. is supported by the Natural Sciences and Engineering Research Council, the Canadian Foundation for Climate and Atmospheric Sciences, and the Canadian Space Agency.

References

Baldwin, M. P., et al. (2001), The quasi-biennial oscillation, *Rev. Geophys.*, *39*, 179–229, doi:10.1029/1999RG000073.

Bhartia, P. K., C. G. Wellemeyer, S. L. Taylor, N. Nath, and A. Gopolan (2004), Solar backscatter ultraviolet (SBUV) version 8 profile algorithm, paper presented at Quadrennial Ozone Symposium, Int. Ozone Comm., Kos, Greece.

Bowman, K. P. (1989), Global patterns of the quasi-biennial oscillation in total ozone, *J. Atmos. Sci.*, *46*, 3328–3343, doi:10.1175/1520-0469(1989)046<3328:GPOTQB>2.0.CO;2.

Brasseur, G., and S. Solomon (2005), *Aeronomy of the Middle Atmosphere*, 2nd ed., Springer, New York.

Chipperfield, M. P., L. J. Gray, J. S. Kinnersley, and J. Zawodny (1994), A two-dimensional model study of the QBO signal in SAGE II NO_2 and O_3, *Geophys. Res. Lett.*, *21*, 589–592, doi:10.1029/94GL00211.

Cunnold, D. M., W. P. Chu, R. A. Barnes, M. P. McCormick, R. E. Veiga, D. Murcray, N. Iwagami, K. Shibasaki, P. C. Simon, and W. Peetermans (1989), Validation of SAGE II ozone measurements, *J. Geophys. Res.*, *94*, 8447–8460, doi:10.1029/JD094iD06p08447.

Fioletov, V. E., and T. G. Shepherd (2003), Seasonal persistence of midlatitude total ozone anomalies, *Geophys. Res. Lett.*, *30*(7), 1417, doi:10.1029/2002GL016739.

Fioletov, V. E., and T. G. Shepherd (2005), Summertime total ozone variations over middle and polar latitudes, *Geophys. Res. Lett.*, *32*, L04807, doi:10.1029/2004GL022080.

Fioletov, V. E., D. W. Tarasick, and I. Petropavlovskikh (2006), Estimating ozone variability and instrument uncertainties from SBUV(/2), ozonesonde, Umkehr, and SAGE II measurements: Short-term variations, *J. Geophys. Res.*, *111*, D02305, doi:10.1029/2005JD006340.

Frith, S., R. Stolarski, and P. K. Bhartia (2004), Implications of version 8 TOMS and SBUV data for long-term trend analysis, paper presented at Quadrennial Ozone Symposium, Int. Ozone Comm., Kos, Greece.

Grooß, J.-U., and J. M. Russell III (2005), Technical note: A stratospheric climatology for O_3, H_2O, CH_4, NO_x, HCl and HF derived from HALOE measurements, *Atmos. Chem. Phys.*, *5*, 2797–2807, doi:10.5194/acp-5-2797-2005.

Hasebe, F. (1994), Quasi-biennial oscillation of ozone and diabatic circulation in the equatorial stratosphere, *J. Atmos. Sci.*, *51*, 729–745, doi:10.1175/1520-0469(1994)051<0729:QBOOOA>2.0.CO;2.

Holton, J. R., and H.-C. Tan (1980), The influence of the equatorial quasi-biennial oscillation on the global circulation at 50 mb, *J. Atmos. Sci.*, *37*, 2200–2208, doi:10.1175/1520-0469(1980)037<2200:TIOTEQ>2.0.CO;2.

Jones, D. B. A., H. R. Schneider, and M. B. McElroy (1998), Effects of the quasi-biennial oscillation on the zonally averaged transport of tracers, *J. Geophys. Res.*, *103*, 11,235–11,249, doi:10.1029/98JD00682.

Ling, X. D., and J. London (1986), The quasi-biennial oscillation of ozone in the tropical middle stratosphere: A one-dimensional model, *J. Atmos. Sci.*, *43*, 3122–3137, doi:10.1175/1520-0469(1986)043<3122:TQBOOO>2.0.CO;2.

McCormick, M. P., J. M. Zawodny, R. E. Veiga, J. C. Larsen, and P.-H. Wang (1989), An overview of SAGE I and II ozone measurements, *Planet. Space Sci.*, *37*, 1567–1586, doi:10.1016/0032-0633(89)90146-3.

McLinden, C. A., S. Tegtmeier, and V. E. Fioletov (2009), Technical note: A combined SBUV and SAGE zonal mean data set, *Atmos. Chem. Phys.*, *9*, 7963–7972, doi:10.5194/acp-9-7963-2009.

Newman, P. A., J. S. Daniel, D. W. Waugh, and E. R. Nash (2007), A new formulation of equivalent effective stratospheric chlorine (EESC), *Atmos. Chem. Phys.*, *7*, 4537–4552, doi:10.5194/acp-7-4537-2007.

Randel, W. J., and J. B. Cobb (1994), Coherent variations of monthly mean total ozone and lower stratospheric temperature, *J. Geophys. Res.*, *99*, 5433–5447, doi:10.1029/93JD03454.

Randel, W. J., and F. Wu (1996), Isolation of the ozone QBO in SAGE II data by singular value decomposition, *J. Atmos. Sci.*, *53*, 2546–2559, doi:10.1175/1520-0469(1996)053<2546:IOTOQI>2.0.CO;2.

Randel, W. J., and F. Wu (2007), A stratospheric ozone profile data set for 1979–2005: Variability, trends, and comparisons with column ozone data, *J. Geophys. Res.*, *112*, D06313, doi:10.1029/2006JD007339.

Russell, J. M., III, L. L. Gordley, J. H. Park, S. R. Drayson, D. H. Hesketh, R. J. Cicerone, A. F. Tuck, J. E. Frederick, J. E. Harries, and P. J. Crutzen (1993), The Halogen Occultation Experiment, *J. Geophys. Res.*, *98*, 10,777–10,797, doi:10.1029/93JD00799.

Semeniuk, K., and T. G. Shepherd (2001), The middle-atmosphere Hadley circulation and equatorial inertial adjustment, *J. Atmos. Sci.*, *58*, 3077–3096, doi:10.1175/1520-0469(2001)058<3077:TMAHCA>2.0.CO;2.

Shepherd, T. G. (2007), Transport in the middle atmosphere, *J. Meteorol. Soc. Jpn.*, *85B*, 165–191, doi:10.2151/jmsj.85B.165.

Tegtmeier, S., and T. G. Shepherd (2007), Persistence and photochemical decay of springtime total ozone anomalies in the Canadian Middle Atmosphere Model, *Atmos. Chem. Phys.*, *7*, 485–493, doi:10.5194/acp-7-485-2007.

Tegtmeier, S., V. E. Fioletov, and T. G. Shepherd (2008), Seasonal persistence of northern low and middle latitude anomalies of ozone and other trace gases in the upper stratosphere, *J. Geophys. Res.*, *113*, D21308, doi:10.1029/2008JD009860.

Tegtmeier, S., V. E. Fioletov, and T. G. Shepherd (2010), Seasonal persistence of ozone and zonal wind anomalies in the equatorial stratosphere, *J. Geophys. Res.*, *115*, D18118, doi:10.1029/2009JD013010.

Tian, W., M. P. Chipperfield, L. J. Gray, and J. M. Zawodny (2006), Quasi-biennial oscillation and tracer distributions in a coupled chemistry-climate model, *J. Geophys. Res.*, *111*, D20301, doi:10.1029/2005JD006871.

Tung, K. K., and H. Yang (1994), Global QBO in circulation and ozone. Part I: Reexamination of observational evidence, *J. Atmos. Sci.*, *51*, 2699–2707, doi:10.1175/1520-0469(1994)051<2699:GQICAO>2.0.CO;2.

Wang, P.-H., D. M. Cunnold, C. R. Trepte, H. J. Wang, P. Jing, J. Fishman, V. G. Brackett, J. M. Zawodny, and G. E. Bodeker (2006), Ozone variability in the midlatitude upper troposphere and lower stratosphere diagnosed from a monthly SAGE II climatology relative to the tropopause, *J. Geophys. Res.*, *111*, D21304, doi:10.1029/2005JD006108.

World Meteorological Organization (2007), WMO scientific assessment of ozone depletion: 2006, *Rep. 50*, Global Ozone Res. and Monit. Proj., Geneva.

Zawodny, J. M., and M. P. McCormick (1991), Stratospheric Aerosol and Gas Experiment II measurements of the quasi-biennial oscillations in ozone and nitrogen dioxide, *J. Geophys. Res.*, *96*, 9371–9377, doi:10.1029/91JD00517.

V. E. Fioletov, Environment Canada, 4905 Dufferin St., Toronto, ON M3H 5T4, Canada.

T. G. Shepherd, Department of Physics, University of Toronto, 60 St. George St., Toronto, ON M5S 1A7, Canada.

S. Tegtmeier, Marine Meteorology, IFM-GEOMAR, Düsternbrooker Weg 20, D-24105 Kiel, Germany. (stegtmeier@ifm-geomar.de)